

Accurate Theory for Thermal Elastic-Plastic Analysis to Significantly Shorten Computation Time[†]

NAKACHO Keiji*

Abstract

The thermal elastic-plastic analysis of the transient and residual stresses and the deformations that occur during welding requires a long computation time to obtain accurate results. The reason for this is the necessity for the temperature increment to be sufficiently small to ensure calculation accuracy. In this study, the thermal elastic and thermal elastic-plastic constitutive equations were modified to enable the use of very large temperature increments. Moreover, in the latter constitutive equation, the definition of the differential coefficient of the yield stress when the temperature changes is ingeniously modified to perfectly satisfy the yield condition. The new constitutive equations were introduced into the FEM (Finite Element Method) program.

A simple typical problem of thermal elastic-plastic mechanics was analyzed to verify the basic capability of the new theory. Further, to examine the reliability and accuracy of the theory, a complex welding problem was analyzed. The computed welding residual stress and deformation were compared with the accurate results obtained by the usual incremental method using very small temperature increments, and those obtained by ABAQUS. High accuracy was confirmed, and the computation was found to be significantly shortened (reduced by one order) compared to those of the usual incremental method and ABAQUS.

KEY WORDS: (thermal elastic-plastic analysis), (shortening of computation time), (refined constitutive equation), (finite element method), (welding stress and deformation)

1. Introduction

The thermal elastic-plastic analysis of the transient and residual stresses and the deformations that occur during welding is done using the incremental method [1–3] because of the non-linear behavior and the dependency on the temperature history. The temperature increment used for the analysis has to be sufficiently small to ensure calculation accuracy. The analysis [4–11] therefore requires long computation time.

In this study, the thermal elastic and thermal elastic-plastic constitutive equations are modified to enable the use of very large temperature increments. Moreover, in the latter constitutive equation, the definition of the differential coefficient of the yield stress when the temperature changes is ingeniously modified to perfectly satisfy the yield condition. The new constitutive equations are effective, simple, and can be easily introduced into the usual FEM (Finite Element Method) program for thermal elastic-plastic analysis.

A simple typical problem of thermal elastic-plastic mechanics was analyzed to verify the basic capability of the new theory. To examine the reliability and accuracy of the theory, a complex welding problem was also

analyzed. The results (the welding residual stress and deformation) were compared with the accurate results obtained by the usual incremental method using a very small temperature increment, and those obtained by ABAQUS.

2. New Accurate Incremental Theory of Thermal Elastic-Plastic Analysis for Large Temperature Increment

The new accurate thermal elastic and thermal elastic-plastic constitutive equations are developed here, and can be used for very large temperature increments.

2.1 Difficulties of Using Large Temperature Increment

The two major reasons why it is difficult to increase the temperature increment during thermal elastic-plastic analyses, especially those of the mechanical phenomena of welding, are as follows:

(a) The material properties change with respect to the temperature and its history. Especially in welding, the temperature range is very wide. The changes in the material properties are therefore significant.

[†] Received on June 30, 2014

* Associate Professor

Transactions of JWRI is published by Joining and Welding Research Institute, Osaka University, Ibaraki, Osaka 567-0047, Japan

(b) When the stress becomes large, the stress state may change from elastic to plastic. In the incremental method, the change occurs incrementally. If the calculation is performed for the elastic state, the equivalent stress after the increment may significantly exceed the yield stress; that is, the stress point may largely fly across the yield surface in the stress space.

To use large temperature increments and maintain high accuracy, these behaviors should be sufficiently considered and managed in the theory.

Regarding problem (a) above, it is necessary to take into account the temperature and its history and how they affect the material properties, regardless of the magnitude of the temperature increment. Moreover, for large temperature increments, the temperature, which determines the material property, becomes more important for accurate analysis.

Regarding problem (b) above, the error that results from going beyond the yield surface is an important issue, especially when large temperature increments are used. The error may increase as the increment increases. Accordingly, if a large temperature increment is used, the theory should include a function that prevents the stress point from exceeding the yield surface during the increment, or a modification function that returns the stress point to the yield surface during the next increment. In this paper, a new theory that includes the latter function will be proposed.

The denotations of the superscripts and subscripts used in equations in subsequent sections are as follows:

- a : initial value in the increment
- c : final value in the increment
- $a - c$: mean value during the increment
- ac : coefficient intermingled of initial, final, and mean values
- $c - a$: incremental value

2.2 Accurate Elastic Constitutive Equation for Large Temperature Increment

A very accurate constitutive equation is derived for the case in which the elastic state is maintained during large temperature increments.

(a) Thermal strain increment $\left\{ d\varepsilon^T \right\}_{c-a}$

$$\left\{ d\varepsilon^T \right\}_{c-a} = \left\{ \alpha \right\}_{a-c} dT_{c-a} \quad (1)$$

where $\left\{ \alpha \right\}_{a-c}$ is the instantaneous linear expansion coefficient, and dT_{c-a} is the temperature increment.

(b) Total strain increment $\left\{ d\varepsilon \right\}_{c-a}$

$$\left\{ d\varepsilon \right\}_{c-a} = \left\{ d\varepsilon^e \right\}_{c-a} + \left\{ d\varepsilon^T \right\}_{c-a} \quad (2)$$

where $\left\{ d\varepsilon^e \right\}_{c-a}$ is the elastic strain increment.

(c) Stress-elastic strain relationship

$$\left\{ \sigma \right\} = \left[D^e(T) \right] \left\{ \varepsilon^e \right\} \quad (3)$$

where $\left\{ \sigma \right\}$ is the stress, $\left\{ \varepsilon^e \right\}$ is the elastic strain, and $\left[D^e(T) \right]$ is the elastic matrix (composed of the Young's modulus and the Poisson's ratio, which are temperature-dependent, and (T) is omitted below).

The most important relationship that must be satisfied at all times in the elastic state and the elastic-plastic state is that between the stress and the elastic strain; that is, Eq. (3). Like Eq. (4), Eq. (3) must be satisfied for all temperatures during the increment.

$$\begin{aligned} \left\{ \sigma \right\}_a &= \left[D^e \right]_a \left\{ \varepsilon^e \right\}_a \\ \left\{ \sigma \right\}_c &= \left[D^e \right]_c \left\{ \varepsilon^e \right\}_c \end{aligned} \quad (4)$$

$$\begin{aligned} \left\{ \sigma \right\}_c &= \left\{ \sigma \right\}_a + \left\{ d\sigma \right\}_{c-a} \\ \left[D^e \right]_c \left\{ \varepsilon^e \right\}_c &= \left(\left[D^e \right]_a + d \left[D^e \right]_{c-a} \right) \left(\left\{ \varepsilon^e \right\}_a + \left\{ d\varepsilon^e \right\}_{c-a} \right) \end{aligned}$$

where $\left\{ d\sigma \right\}_{c-a}$ is the stress increment, and

$$d \left[D^e \right]_{c-a} = d \left[D^e \right]_c - d \left[D^e \right]_a = \left(\frac{\left[D^e \right]_c - \left[D^e \right]_a}{dT_{c-a}} \right) dT_{c-a} = \left(\frac{d \left[D^e \right]}{dT} \right)_{ac} dT_{c-a} \quad (5)$$

The relationship between the stress increment and the elastic strain increment is obtained from Eq. (4).

$$\left\{ d\sigma \right\}_{c-a} = \left[D^e \right]_c \left\{ d\varepsilon^e \right\}_{c-a} + d \left[D^e \right]_{c-a} \left\{ \varepsilon^e \right\}_a \quad (6)$$

(d) Incremental stress-total strain relationship (the elastic constitutive equation)

The incremental constitutive equation for the elastic state is derived from Eqs. (1), (2), and (6). Equation (7) is the accurate elastic constitutive equation, which sufficiently considers the temperatures required to determine the material properties. Using Eq. (7), Eq. (3) is satisfied after the increment, even if the temperature increment is very large.

$$\left\{ d\sigma \right\}_{c-a} = \left[D^e \right]_c \left\{ d\varepsilon \right\}_{c-a} - \left\{ C^e \right\}_{ac} dT_{c-a} \quad (7)$$

where

$$\left\{ C^e \right\}_{ac} = \left[D^e \right]_c \left(\left\{ \alpha \right\}_{a-c} - \left[D^e \right]_c^{-1} \left(\frac{d \left[D^e \right]}{dT} \right)_{ac} \left\{ \varepsilon^e \right\}_a \right)$$

2.3 Accurate Elastic-Plastic Constitutive Equation for Large Temperature Increment

A very accurate constitutive equation is derived for the case in which the elastic-plastic state is maintained during a large temperature increment.

(a) Total strain increment $\{d\varepsilon\}_{c-a}$

$$\{d\varepsilon\}_{c-a} = \{d\varepsilon^e\}_{c-a} + \{d\varepsilon^p\}_{c-a} + \{d\varepsilon^T\}_{c-a} \quad (8)$$

where $\{d\varepsilon^p\}_{c-a}$ is the plastic strain increment.

(b) Yield function (strain-hardening rule) $f(\sigma_{ij} - \theta_{ij}, \sigma_o)$

In this theory, the incremental strain theory (the flow theory) is assumed, and the combined strain-hardening rule is applied to the yield function, in which the yield surface can change both the size and the position. The size of the yield surface depends on the total plastic strain and the temperature. The yield surface (yield condition) and the change of in size are related by

$$f(\sigma_{ij} - \theta_{ij}, \sigma_o) = 0 \quad (9)$$

where $\{\theta\}$ is the center of the yield surface, σ_o is the size of the yield surface, $\sigma_o = \sigma_o(\bar{\varepsilon}^p, T)$, and $\bar{\varepsilon}^p$ is the magnitude of the total plastic strain given by $\bar{\varepsilon}^p = \sum d\bar{\varepsilon}^p$ ($d\bar{\varepsilon}^p$ is the magnitude of the plastic strain increment, and see Eq. (14)).

$$d\sigma_{o,c-a} = \left(\frac{\partial\sigma_o}{\partial T}\right)_a dT_{c-a} + \left(\frac{\partial\sigma_o}{\partial\bar{\varepsilon}^p}\right)_a d\bar{\varepsilon}^p_{c-a} \quad (10)$$

Because the temperature dependence of σ_o has been obtained by a previous material experiment, the differential coefficient in the first term on the right side of Eq. (10) is redefined as Eq. (11) to improve the accuracy for a large temperature increment. The differentiation is transformed into the difference that produces the true change. Equation (10) is then modified to Eq. (12).

$$\left(\frac{\partial\sigma_o}{\partial T}\right)_{ac} = \frac{\sigma_o(\bar{\varepsilon}^p_a, T_c) - \sigma_o(\bar{\varepsilon}^p_a, T_a)}{dT_{c-a}} \quad (11)$$

$$d\sigma_{o,c-a} = \left(\frac{\partial\sigma_o}{\partial T}\right)_{ac} dT_{c-a} + \left(\frac{\partial\sigma_o}{\partial\bar{\varepsilon}^p}\right)_a d\bar{\varepsilon}^p_{c-a} \quad (12)$$

Assuming that the magnitude of the movement of the yield surface is proportional to the magnitude of the plastic strain increment,

$$\{d\theta\}_{c-a} = k d\bar{\varepsilon}^p_{c-a} \{n_\theta\}_a \quad (13)$$

where k is the coefficient of proportionality, $d\bar{\varepsilon}^p_{c-a}$ is the magnitude of the plastic strain increment (see Eq. (14)), and $\{n_\theta\}_a$ is the unit vector that indicates the direction of the yield surface movement and can be freely assumed (for example, by the Ziegler rule).

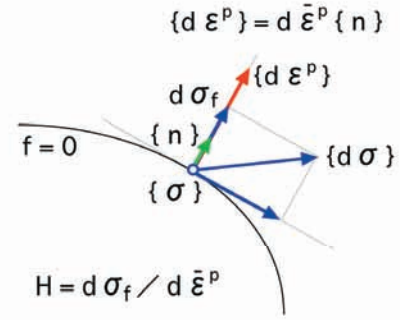


Fig. 1 Definition of strain-hardening coefficient (Relation between stress increment and plastic strain increment)

(c) Plastic strain increment $\{d\varepsilon^p\}_{c-a}$

Assuming the incremental strain theory (the flow theory), the plastic strain increment is defined as follows, and its direction is perpendicular to the plastic potential (the yield surface) as shown in **Fig. 1**:

$$\{d\varepsilon^p\}_{c-a} = d\bar{\varepsilon}^p_{c-a} \{n\}_a \quad (14)$$

where $d\bar{\varepsilon}^p_{c-a}$ is the magnitude of the plastic strain increment, and $\{n\}_a$ is the outward unit vector normal to the yield surface at the stress point.

$$\{n\}_a = \left\{ \frac{\partial f}{\partial(\sigma - \theta)} \right\}_a / f_{\sigma\theta,a} \quad (15)$$

$$f_{\sigma\theta,a} = \left| \left\{ \frac{\partial f}{\partial(\sigma - \theta)} \right\}_a \right| = \left(\left\{ \frac{\partial f}{\partial(\sigma - \theta)} \right\}_a^T \left\{ \frac{\partial f}{\partial(\sigma - \theta)} \right\}_a \right)^{1/2}$$

(d) Strain-hardening coefficient H_{ac}

The strain-hardening coefficient is defined as the ratio of the normal component of the stress increment to the magnitude of the plastic strain increment as expressed by Eq. (16) and shown in Fig. 1, and it depends on the total plastic strain and the temperature. The temperature is not T_a but T_c because the yield condition should be satisfied after the increment (this will be explained in detail in Sec. 2.5 using **Fig. 2**). The relationship between H and $\bar{\varepsilon}^p$ can be obtained by material experiments conducted at various temperatures T .

$$H_{ac} = \frac{d\sigma_{f,c-a}}{d\bar{\varepsilon}^p_{c-a}} = H(\bar{\varepsilon}^p_a, T_c) \quad (16)$$

where $d\sigma_{f,c-a}$ is the normal component of $\{d\sigma\}_{c-a}$, and

$$d\sigma_{f,c-a} = \{n\}_a^T \{d\sigma\}_{c-a} \quad (17)$$

(e) Proportionality coefficient k in $\{d\theta\}_{c-a}$

The consistency condition for Eq. (9) for each increment is expressed below.

$$df(\sigma_{ij} - \theta_{ij}, \sigma_o)_{c-a} = \left\{ \frac{\partial f}{\partial(\sigma - \theta)} \right\}_a^T \{d(\sigma - \theta)\}_{c-a} + \left(\frac{\partial f}{\partial \sigma_o} \right)_a d\sigma_{o,c-a} = 0 \quad (18)$$

When the combined strain-hardening rule is applied and the consistency condition is satisfied, the relationship between the proportionality coefficient k in $\{d\theta\}_{c-a}$ and the strain-hardening coefficient H_{ac} is obtained as follows.

From Eq. (18),

$$\left\{ \frac{\partial f}{\partial(\sigma - \theta)} \right\}_a^T \{d(\sigma - \theta)\}_{c-a} = - \left(\frac{\partial f}{\partial \sigma_o} \right)_a d\sigma_{o,c-a}$$

Equations (15) and (12) are substituted into the above equation.

$$\begin{aligned} f_{\sigma\theta,a} \{n\}_a^T \{d\sigma\}_{c-a} - \{d\theta\}_{c-a} &= - \left(\frac{\partial f}{\partial \sigma_o} \right)_a \left[\left(\frac{\partial \sigma_o}{\partial T} \right)_{ac} dT_{c-a} + \left(\frac{\partial \sigma_o}{\partial \bar{\varepsilon}^p} \right)_a d\bar{\varepsilon}^p_{c-a} \right] \\ f_{\sigma\theta,a} \{n\}_a^T \{d\sigma\}_{c-a} - f_{\sigma\theta,a} \{n\}_a^T \{d\theta\}_{c-a} &= - \left(\frac{\partial f}{\partial \sigma_o} \right)_a \left(\frac{\partial \sigma_o}{\partial T} \right)_{ac} dT_{c-a} - \left(\frac{\partial f}{\partial \sigma_o} \right)_a \left(\frac{\partial \sigma_o}{\partial \bar{\varepsilon}^p} \right)_a d\bar{\varepsilon}^p_{c-a} \end{aligned} \quad (19)$$

Equations (17) and (13) are substituted into the above equation.

$$\begin{aligned} f_{\sigma\theta,a} d\sigma_{f,c-a} - f_{\sigma\theta,a} \{n\}_a^T k d\bar{\varepsilon}^p_{c-a} \{n_\theta\}_a &= - \left(\frac{\partial f}{\partial \sigma_o} \right)_a \left(\frac{\partial \sigma_o}{\partial T} \right)_{ac} dT_{c-a} - \left(\frac{\partial f}{\partial \sigma_o} \right)_a \left(\frac{\partial \sigma_o}{\partial \bar{\varepsilon}^p} \right)_a d\bar{\varepsilon}^p_{c-a} \\ d\sigma_{f,c-a} &= k d\bar{\varepsilon}^p_{c-a} n_{\theta f,a} - \frac{1}{f_{\sigma\theta,a}} \left(\frac{\partial f}{\partial \sigma_o} \right)_a \left(\frac{\partial \sigma_o}{\partial T} \right)_{ac} dT_{c-a} - \frac{1}{f_{\sigma\theta,a}} \left(\frac{\partial f}{\partial \sigma_o} \right)_a \left(\frac{\partial \sigma_o}{\partial \bar{\varepsilon}^p} \right)_a d\bar{\varepsilon}^p_{c-a} \\ d\sigma_{f,c-a} &= \left(k n_{\theta f,a} - \frac{1}{f_{\sigma\theta,a}} \left(\frac{\partial f}{\partial \sigma_o} \right)_a \left(\frac{\partial \sigma_o}{\partial \bar{\varepsilon}^p} \right)_a \right) d\bar{\varepsilon}^p_{c-a} - \frac{1}{f_{\sigma\theta,a}} \left(\frac{\partial f}{\partial \sigma_o} \right)_a \left(\frac{\partial \sigma_o}{\partial T} \right)_{ac} dT_{c-a} \end{aligned} \quad (20)$$

where $n_{\theta f,a}$ is the normal component of $\{n_\theta\}_a$,

$$n_{\theta f,a} = \{n\}_a^T \{n_\theta\}_a$$

Equation (20) is substituted into Eq. (16).

$$H_{ac} = \frac{d\sigma_{f,c-a}}{d\bar{\varepsilon}^p_{c-a}} = k n_{\theta f,a} - 0 - \frac{1}{f_{\sigma\theta,a}} \left(\frac{\partial f}{\partial \sigma_o} \right)_a \left(\frac{\partial \sigma_o}{\partial \bar{\varepsilon}^p} \right)_a = k n_{\theta f,a} - \frac{1}{f_{\sigma\theta,a}} \left(\frac{\partial f}{\partial \sigma_o} \right)_a \left(\frac{\partial \sigma_o}{\partial \bar{\varepsilon}^p} \right)_a \quad (21)$$

The coefficient k can be calculated using Eq. (21) because the strain-hardening coefficient H_{ac} has been determined in advance by a material experiment.

(f) Magnitude $d\bar{\varepsilon}^p_{c-a}$ of plastic strain increment $\{d\varepsilon^p\}_{c-a}$

From Eq. (6),

$$\{n\}_a^T \{d\sigma\}_{c-a} = \{n\}_a^T [D^e]_c \{d\varepsilon^e\}_{c-a} + \{n\}_a^T d[D^e]_{c-a} \{\varepsilon^e\}_a \quad (22)$$

From Eqs. (20) and (21),

$$\begin{aligned} \{n\}_a^T \{d\sigma\}_{c-a} &= d\sigma_{f,c-a} = \left(k n_{\theta f,a} - \frac{1}{f_{\sigma\theta,a}} \left(\frac{\partial f}{\partial \sigma_o} \right)_a \left(\frac{\partial \sigma_o}{\partial \bar{\varepsilon}^p} \right)_a \right) d\bar{\varepsilon}^p_{c-a} - \frac{1}{f_{\sigma\theta,a}} \left(\frac{\partial f}{\partial \sigma_o} \right)_a \left(\frac{\partial \sigma_o}{\partial T} \right)_{ac} dT_{c-a} \\ &= H_{ac} d\bar{\varepsilon}^p_{c-a} - \frac{1}{f_{\sigma\theta,a}} \left(\frac{\partial f}{\partial \sigma_o} \right)_a \left(\frac{\partial \sigma_o}{\partial T} \right)_{ac} dT_{c-a} \end{aligned} \quad (23)$$

From Eqs. (22) and (23),

$$\{n\}_a^T [D^e]_c \{d\varepsilon^e\}_{c-a} + \{n\}_a^T d[D^e]_{c-a} \{\varepsilon^e\}_a = H_{ac} d\bar{\varepsilon}^p_{c-a} - \frac{1}{f_{\sigma\theta,a}} \left(\frac{\partial f}{\partial \sigma_o} \right)_a \left(\frac{\partial \sigma_o}{\partial T} \right)_{ac} dT_{c-a} \quad (24)$$

From Eq. (8),

$$\{d\varepsilon^e\}_{c-a} = \{d\varepsilon\}_{c-a} - \{d\varepsilon^p\}_{c-a} - \{d\varepsilon^T\}_{c-a} \quad (25)$$

Equation (25) is substituted into Eq. (24).

$$\begin{aligned} \{n\}_a^T [D^e]_c \left(\{d\varepsilon\}_{c-a} - \{d\varepsilon^p\}_{c-a} - \{d\varepsilon^T\}_{c-a} \right) + \{n\}_a^T d[D^e]_{c-a} \{\varepsilon^e\}_a \\ = H_{ac} d\bar{\varepsilon}^p_{c-a} - \frac{1}{f_{\sigma\theta,a}} \left(\frac{\partial f}{\partial \sigma_o} \right)_a \left(\frac{\partial \sigma_o}{\partial T} \right)_{ac} dT_{c-a} \end{aligned} \quad (26)$$

Equations (1) and (14) are substituted into Eq. (26).

$$\begin{aligned} \{n\}_a^T [D^e]_c \left(\{d\varepsilon\}_{c-a} - d\bar{\varepsilon}^p_{c-a} \{n\}_a - \{\alpha\}_{a-c} dT_{c-a} \right) + \{n\}_a^T d[D^e]_{c-a} \{\varepsilon^e\}_a \\ = H_{ac} d\bar{\varepsilon}^p_{c-a} - \frac{1}{f_{\sigma\theta,a}} \left(\frac{\partial f}{\partial \sigma_o} \right)_a \left(\frac{\partial \sigma_o}{\partial T} \right)_{ac} dT_{c-a} \end{aligned}$$

$$\begin{aligned} \{n\}_a^T [D^e]_c \{d\varepsilon\}_{c-a} \\ - \left\{ \{n\}_a^T [D^e]_c \{\alpha\}_{a-c} - \{n\}_a^T d[D^e]_{c-a} \{\varepsilon^e\}_a / dT_{c-a} - \frac{1}{f_{\sigma\theta,a}} \left(\frac{\partial f}{\partial \sigma_o} \right)_a \left(\frac{\partial \sigma_o}{\partial T} \right)_{ac} \right\} dT_{c-a} \\ = \left(\{n\}_a^T [D^e]_c \{n\}_a + H_{ac} \right) d\bar{\varepsilon}^p_{c-a} \end{aligned} \quad (27)$$

From Eqs. (27) and (5),

$$\begin{aligned} \{n\}_a^T [D^e]_c \{d\varepsilon\}_{c-a} \\ - \left\{ \{n\}_a^T [D^e]_c \{\alpha\}_{a-c} - \{n\}_a^T \left(\frac{d[D^e]}{dT} \right)_{ac} \{\varepsilon^e\}_a - \frac{1}{f_{\sigma\theta,a}} \left(\frac{\partial f}{\partial \sigma_o} \right)_a \left(\frac{\partial \sigma_o}{\partial T} \right)_{ac} \right\} dT_{c-a} \\ = \left(\{n\}_a^T [D^e]_c \{n\}_a + H_{ac} \right) d\bar{\varepsilon}^p_{c-a} \end{aligned}$$

$$\begin{aligned} & \{n\}_a^T [D^e]_c \{d\varepsilon\}_{c-a} \\ & - \left\{ \{n\}_a^T [D^e]_c \left(\{\alpha\}_{a-c} - [D^e]_c^{-1} \left(\frac{d[D^e]}{dT} \right) \{ \varepsilon^e \}_a \right) - \frac{1}{f_{\sigma\theta,a}} \left(\frac{\partial f}{\partial \sigma_o} \right)_a \left(\frac{\partial \sigma_o}{\partial T} \right)_{ac} \right\} dT_{c-a} \\ & = \left\{ \{n\}_a^T [D^e]_c \{n\}_a + H_{ac} \right\} d\bar{\varepsilon}^p_{c-a} \end{aligned}$$

$$\begin{aligned} d\bar{\varepsilon}^p_{c-a} & = \{n\}_a^T [D^e]_c \{d\varepsilon\}_{c-a} \frac{1}{S_{ac}} \\ & - \left\{ \{n\}_a^T [D^e]_c \left(\{\alpha\}_{a-c} - [D^e]_c^{-1} \left(\frac{d[D^e]}{dT} \right) \{ \varepsilon^e \}_a \right) - \frac{1}{f_{\sigma\theta,a}} \left(\frac{\partial f}{\partial \sigma_o} \right)_a \left(\frac{\partial \sigma_o}{\partial T} \right)_{ac} \right\} \frac{dT_{c-a}}{S_{ac}} \end{aligned} \quad (28)$$

where $S_{ac} = \{n\}_a^T [D^e]_c \{n\}_a + H_{ac}$

Equation (28) expresses the relationship between the total strain increment $\{d\varepsilon\}_{c-a}$ and the magnitude of the plastic strain increment $d\bar{\varepsilon}^p_{c-a}$.

(g) Incremental stress-total strain relationship (the elastic-plastic constitutive equation)

Equation (25) is substituted into Eq. (6).

$$\{d\sigma\}_{c-a} = [D^e]_c \left(\{d\varepsilon\}_{c-a} - \{d\varepsilon^p\}_{c-a} - \{d\varepsilon^T\}_{c-a} \right) + d[D^e]_{c-a} \{ \varepsilon^e \}_a \quad (29)$$

Equations (1), (14), and (28) are substituted into Eq. (29).

$$\{d\varepsilon^T\}_{c-a} = \{\alpha\}_{a-c} dT_{c-a} \quad (1) \text{ bis}$$

$$\{d\varepsilon^p\}_{c-a} = d\bar{\varepsilon}^p_{c-a} \{n\}_a \quad (14) \text{ bis}$$

$$\begin{aligned} d\bar{\varepsilon}^p_{c-a} & = \{n\}_a^T [D^e]_c \{d\varepsilon\}_{c-a} \frac{1}{S_{ac}} \\ & - \left\{ \{n\}_a^T [D^e]_c \left(\{\alpha\}_{a-c} - [D^e]_c^{-1} \left(\frac{d[D^e]}{dT} \right) \{ \varepsilon^e \}_a \right) - \frac{1}{f_{\sigma\theta,a}} \left(\frac{\partial f}{\partial \sigma_o} \right)_a \left(\frac{\partial \sigma_o}{\partial T} \right)_{ac} \right\} \frac{dT_{c-a}}{S_{ac}} \end{aligned} \quad (28) \text{ bis}$$

When the equation is simplified after the substitution, the elastic-plastic constitutive equation (incremental stress-total strain relationship) is obtained as follows:

$$\{d\sigma\}_{c-a} = [D^{ep}]_{ac} \{d\varepsilon\}_{c-a} - \{C^{ep}\}_{ac} dT_{c-a} \quad (30)$$

where $[D^{ep}]_{ac}$ is the elastic-plastic matrix (composed of the temperature-dependent material properties of the elastic and plastic),

$$[D^{ep}]_{ac} = [D^e]_c - [D^e]_c \{n\}_a \{n\}_a^T [D^e]_c \frac{1}{S_{ac}}$$

$$\begin{aligned} \{C^{ep}\}_{ac} & = [D^{ep}]_{ac} \left\{ \{\alpha\}_{a-c} - [D^e]_c^{-1} \left(\frac{d[D^e]}{dT} \right) \{ \varepsilon^e \}_a \right\} \\ & + [D^e]_c \{n\}_a \frac{1}{f_{\sigma\theta,a}} \left(\frac{\partial f}{\partial \sigma_o} \right)_a \left(\frac{\partial \sigma_o}{\partial T} \right)_{ac} \frac{1}{S_{ac}} \end{aligned}$$

When Eq. (30) is used, Eq. (3) is satisfied after the increment, even if the temperature increment is very large.

2.4 Summary of Treatments of Temperature-Dependencies of Mechanical Properties for Large Temperature Increment

The important treatments of the temperature-dependencies of the mechanical properties are summarized here. They are very important, especially when a large temperature increment is used.

(a) For the elastic matrix $[D^e]$ (Young's modulus and Poisson's ratio), the values for the final temperature of the increment (that is, $[D^e]_c$) should be used.

(b) The differential coefficient $d[D^e]/dT$ of $[D^e]$ for the temperature change should be calculated using $[D^e]_a$ and $[D^e]_c$ at the initial and final temperatures of the increment, as expressed by Eq. (5).

(c) For the instantaneous linear expansion coefficient $\{\alpha\}$, the mean value during the increment should be used.

(d) The strain-hardening coefficient H_{ac} has to be determined for the total plastic strain $\bar{\varepsilon}^p_a$ (in the initial state of the increment) and the temperature T_c (the final temperature of the increment), as expressed by Eq. (16). The yield condition will then be definitely satisfied after the increment (this will be explained in detail in Sec. 2.5 using Fig. 2).

2.5 Modifier to Satisfy Yield Condition

When the stress point is on the yield surface and the yield condition is satisfied, the above elastic-plastic constitutive equation (Eq. (30)) can be used for the next temperature increment and can produce accurate results, even for a large temperature increment. However, when the stress point is considerably beyond the yield surface because of using a large temperature increment for the elastic calculation, Eq. (30) will not be necessarily appropriate and may increase the error in the next increment. Hence, a clever method was developed for returning the stress point to the yield surface to satisfy the yield condition during the next increment.

The above elastic-plastic constitutive equation (Eq. (30)) includes the coefficients for considering the effects of the temperature change. One of the coefficients is the

temperature change differential coefficient of σ_o , which is given by Eq. (11). This coefficient is useful and powerful for modifying the stress state.

The differential coefficient $(\partial\sigma_o/\partial T)_{ac}$ is defined by Eq. (11) and is very accurate for a large temperature increment. This coefficient is aptly redefined as follows to return the stress point to the yield surface. On the right side of the equation, the size of the yield surface in the initial state of the increment, $\sigma_o(\bar{\epsilon}_a^p, T_a)$, is changed to the actual equivalent stress in the initial state of the increment, $\bar{\sigma}_a$.

$$\begin{aligned} \left(\frac{\partial\sigma_o}{\partial T}\right)_{ac} &= \frac{\sigma_o(\bar{\epsilon}_a^p, T_c) - \sigma_o(\bar{\epsilon}_a^p, T_a)}{dT_{c-a}} \\ \Rightarrow \left(\frac{\partial\sigma_o}{\partial T}\right)_{ac} &= \frac{\sigma_o(\bar{\epsilon}_a^p, T_c) - \bar{\sigma}_a}{dT_{c-a}} \end{aligned} \quad (31)$$

The constitutive equation (Eq. (30)) is basically used. However, only the coefficient $(\partial\sigma_o/\partial T)_{ac}$ in the equation is changed from Eq. (11) to Eq. (31).

The effect of the new definition—that is, the mechanism of the modification—will be explained using Fig. 2. To facilitate understanding, it is assumed that the strain-hardening obeys the isotropic hardening rule. The size of the yield surface (the magnitude of the yield stress) is therefore dependent on the total plastic strain and the temperature as shown in Fig. 2.

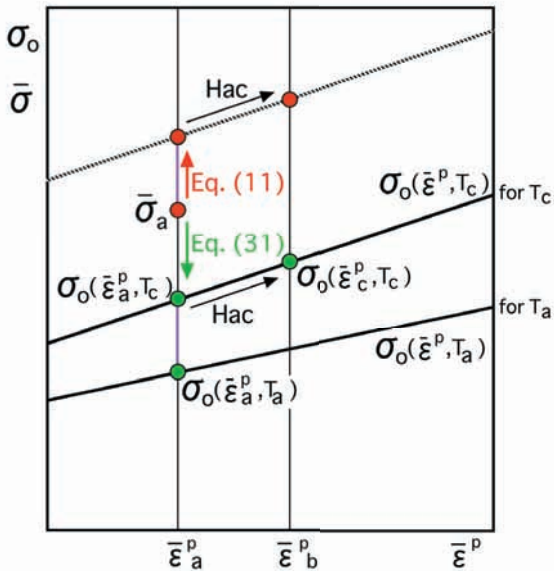


Fig. 2 Mechanism of modification of stress state for yield condition

When the stress point is inside the yield surface, the calculation for the next increment is performed assuming an elastic state. Consequently, the stress point may move outside the yield surface after the increment, especially when a large temperature increment is used. The equivalent stress $\bar{\sigma}_a$ in Fig. 2 shows the stress point in such a situation at temperature T_a . $\bar{\sigma}_a$ is significantly beyond the true yield stress $\sigma_o(\bar{\epsilon}_a^p, T_a)$. The calculation

for the next increment is performed assuming an elastic-plastic. If the plastic state is maintained and Eq. (11) is used, the change of the stress point is given by Eq. (11) + H_{ac} , as shown in Fig. 2, owing to the temperature change and strain-hardening. After the increment, the adverse condition remains. If Eq. (31) is used, the change of the stress point is given by Eq. (31), as shown in Fig. 2, owing to the temperature change. The changed stress point corresponds to $\sigma_o(\bar{\epsilon}_a^p, T_c)$, which is the yield stress

for the total plastic strain $\bar{\epsilon}_a^p$ (in the initial state of the increment) at temperature T_c (the final temperature of the increment). If the plastic strain is additionally produced in the increment, the stress point changes, obeying H_{ac} . In any case, the stress point after the increment is on the yield surface and satisfies the yield condition. However, the final temperature increment must be sufficiently small. If the stress point moves outside the yield surface, the modifier would not work because there would be no subsequent increment.

3. Accuracy and Computation Time of Analysis Using New Theory

3.1 Typical Simple Thermal Elastic-Plastic Problem

To verify the basic capability of the new theory, a typical simple thermal elastic-plastic problem was analyzed. A bar was restrained at both ends as shown in Fig. 3. The thermal stress generated in the bar was analyzed. The material properties are shown in Fig. 4. Both ends of the bar were fixed only at the bottom and the top could slide up and down. This restraint condition produced only axial stress (x-direction stress) and perpendicular deformation (y-direction deformation).

The initial temperature of the bar was uniformly 15°C. The bar was heated to 415°C and subsequently cooled to 15°C while maintaining the temperature uniformity. For the calculation, the heating stage was divided into two increments and the cooling stage into three increments. The temperature increments were therefore 200°C or 100°C. These are very large increments that cannot be used for the usual thermal elastic-plastic analysis if accurate results are required. The analytical results are shown in Fig. 5.

In the heating stage, the first increment was calculated with the assumption of an elastic state using the elastic constitutive equation (Eq. (7)). Consequently, the compressive stress generated in the bar was significantly

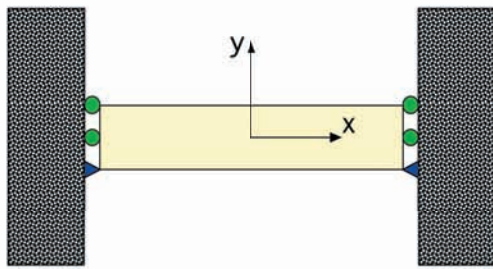


Fig. 3 Restrained bar for analysis

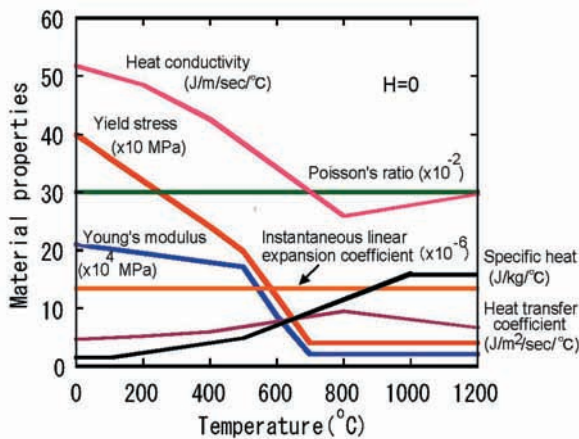


Fig. 4 Temperature dependencies of material properties

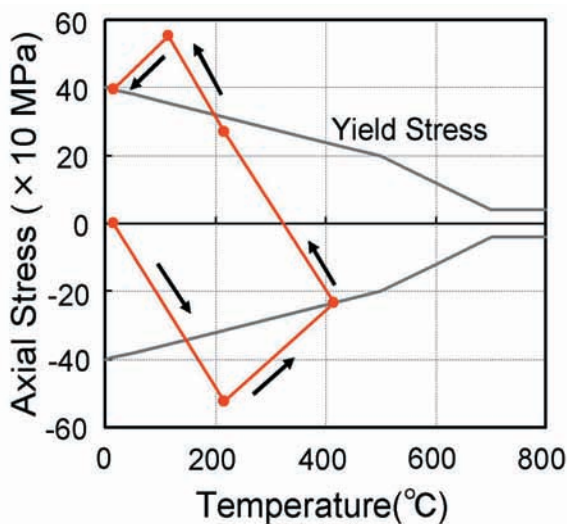


Fig. 5 History of axial stress in bar

beyond the yield stress. The second increment was calculated with the assumption of an elastic-plastic state using the constitutive equation (Eq. (30)) modified by Eq. (31). Consequently, the stress in the bar was adjusted and perfectly corresponded to the yield stress at 415°C.

In the cooling stage, the bar was unloaded in the first increment. The stress became tensile within the yield stress. The second increment was therefore calculated

with the assumption of an elastic state. Consequently, the tensile stress after the increment was significantly beyond the yield stress. The third increment was calculated with the assumption of an elastic-plastic state using Eq. (30) modified by Eq. (31). Consequently, the residual stress perfectly corresponded to the yield stress at 15°C.

As in the stress history, the deformation of the bar—that is, the displacement of the upper side of the bar—corresponded to the exact deformation after application of the modifier.

These results show that the new constitutive equations can be basically used for accurate analysis of the thermal elastic-plastic problem, even when the temperature increments are large.

3.2 Analysis of Welding Residual Stress and Deformation

A typical welding problem was analyzed to verify the capability of the new theory for the analysis of welding stress and deformation. The analysis was done using two theories, namely

(i) The usual accurate incremental theory (hereafter called “usual theory”), which considers the temperature-dependencies of the mechanical properties described in Sec. 2.4, but using Eq. (11) instead of the modifier of Eq. (31).

(ii) The new accurate incremental theory (hereafter called “new theory”) using the modifier of Eq. (31).

By changing the magnitude of the temperature increment, the results of the two theories were examined with regard to their accuracies and computation times (the numbers of increments). Additionally, ABAQUS, which is one of the reliable and globally used commercial solvers, was used to verify the accuracy and effectiveness of the new theory. The CPU computation time was dependent on the performance of the computer. The comparison of the computation times is therefore based on their ratios.

3.2.1 Specimen and welding condition

The specimen used for the analysis is shown in Fig. 6; it has the same dimensions as a “slit cracking test specimen,” which is one of the standard Japanese test

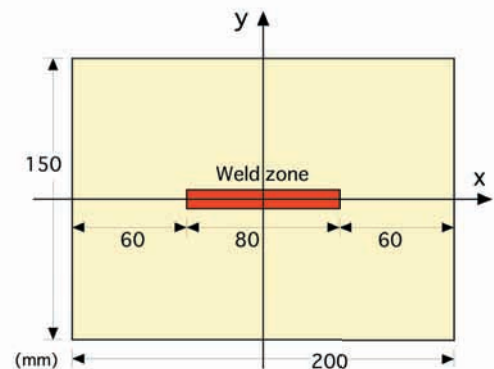


Fig. 6 Specimen used for analysis (slit cracking test specimen)

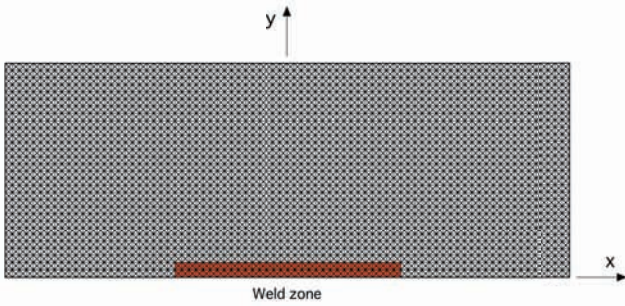


Fig. 7 Mesh division of specimen for FEM

specimens. The welding was done in the slit zone from $x = -40$ mm to $x = +40$ mm. The welding was done under standard Japanese welding conditions, namely 170 A, 25 V, and 15 cm/min (17000 J/cm). In the actual analysis, the specimen did not have a slit; that is, the plate did not have a groove. The heat source with the above conditions moved along the weld zone of the specimen and melted the material as in bead-on-plate welding.

The analysis model represented half of the specimen because of its symmetrical shape and the weld zone. The mesh was divided as shown in Fig. 7; a simple regular division was used because the purpose of the analysis was to examine the performance of the new theory. The numbers of elements, nodes, and unknowns were 9600, 4911, and 9711, respectively.

The material properties were assumed to be the same as in Fig. 4. The mechanical melting point was set at 700°C. At this temperature, the material almost loses its rigidity. At high temperatures above 700°C, the mechanical behavior is unstable and the theoretical analysis may lose stability, especially when large temperature increments are used. Welding involves such high temperatures. The new theory was tested under such adverse conditions.

3.2.2 Analytical results (verification of capability of new theory)

First, the history of the temperature distribution produced by the welding (heat input) was analyzed using the physical properties shown in Fig. 4. The transient temperature distribution obtained from the analysis was divided into 4800 increments, which produced sufficiently small temperature changes (the largest was less than 2.5°C) for accurate thermal stress analysis. The data of the transient temperature distribution with 4800 increments was used for the first thermal stress analysis. The results were accurate and used as benchmark for the problem. Skipping the transient temperature distributions, the number of increments for the thermal stress analysis was decreased from 4800 to 20, which produced very large temperature increments. The analytical results were compared and the residual stress and deformation distributions were noted.

(1) Residual stress

The residual stress distributions along the x-axis are shown in Figs. 8-11. Figures 8 and 9 show the results obtained by the usual theory. Figures 10 and 11 show the results obtained by the new theory. The stresses in the x- and y-direction are represented by σ_x and σ_y , respectively. The symbol U indicates the usual theory, and M the new theory using the modifier. The number beside the symbol indicates the number of increments. Where the black curve for 4800 increments (the benchmark) is not visible, it is under the violet curve (the result for fewer increments).

In the case of 4800 increments, the results obtained by both theories were almost identical. When the number of increments was decreased (that is, larger temperature increments were used), the differences between both results increased.

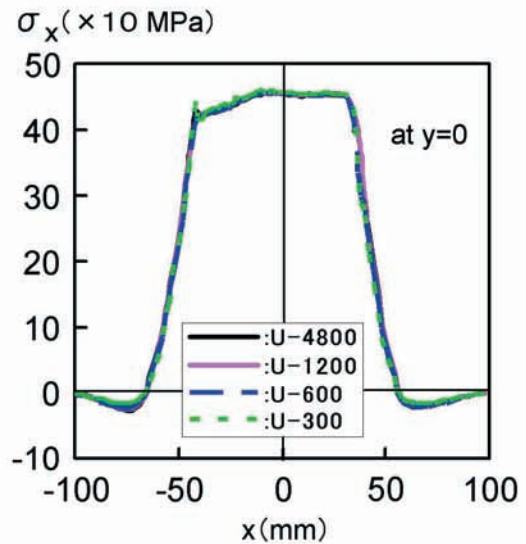


Fig. 8 Residual stress σ_x (by usual accurate theory)

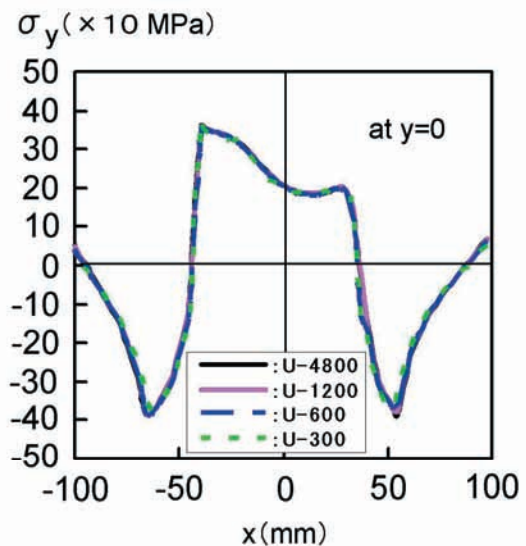


Fig. 9 Residual stress σ_y (by usual accurate theory)

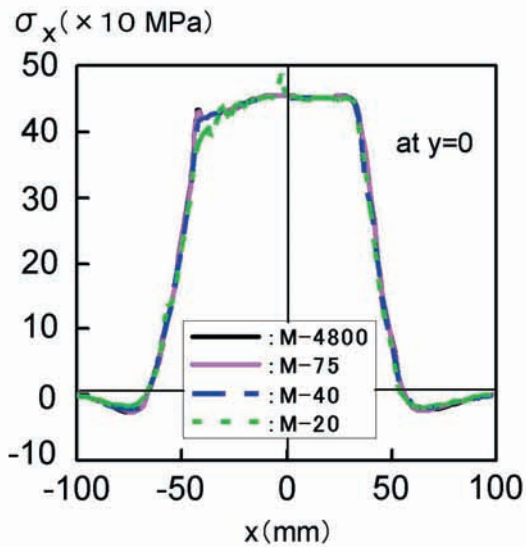


Fig. 10 Residual stress σ_x (by new accurate method)

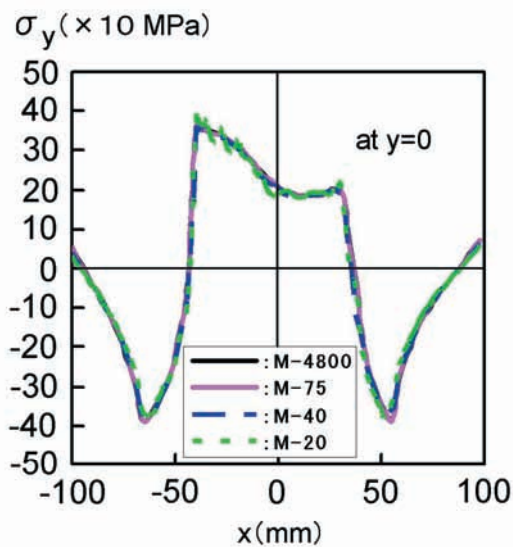


Fig. 11 Residual stress σ_y (by new accurate method)

The accuracy of the usual theory obviously reduces below 1200 increments (the largest temperature increment was about 10°C). Using the new theory, the high accuracy was maintained even when the number of increments was reduced to only 75 (the largest temperature increment was about 150°C). The computation time for an increment was the same for two theories. The computation time using the new theory was therefore shortened to about 6.25% that of the usual theory.

The same welding problem was analyzed using ABAQUS. The temperature data for 4800 increments was also used. ABAQUS automatically decreased the number of increments by increasing the temperature increment while maintaining accuracy. The number of increments

was then reduced to 415. The analytical results were almost identical with those obtained by the above two theories using 4800 increments. The computation time of ABAQUS was about 7.2 times that of the new theory.

(2) Residual deformation

The distributions of the residual deformation along the side of the specimen (from $x = -100$ mm to $x = 100$ mm at $y = 75$ mm) are shown in Figs. 12-15. Figures 12 and 13 show the results obtained by the usual theory. Figures 14 and 15 show the results obtained by the new theory. The displacements in the x- and y-direction are represented by δ_x and δ_y , respectively.

The accuracy of the usual theory was maintained down to 1200 increments, and the corresponding number

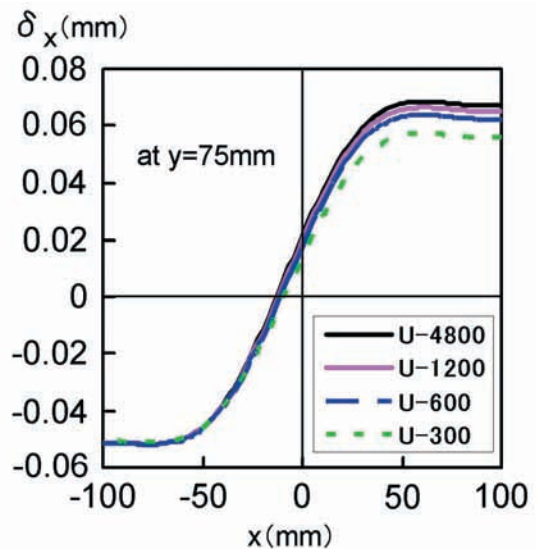


Fig. 12 Residual deformation δ_x (by usual accurate theory)

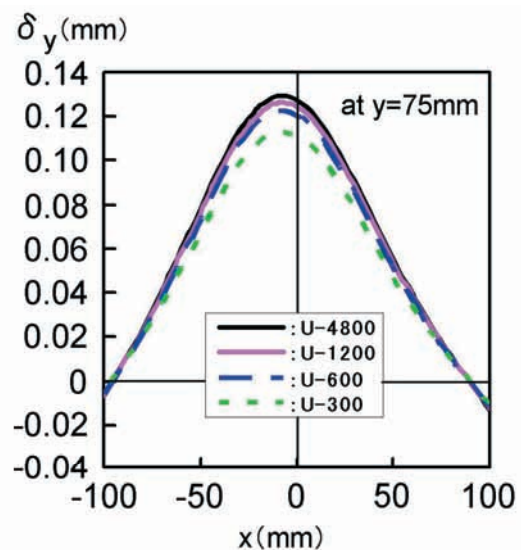


Fig. 13 Residual deformation δ_y (by usual accurate theory)

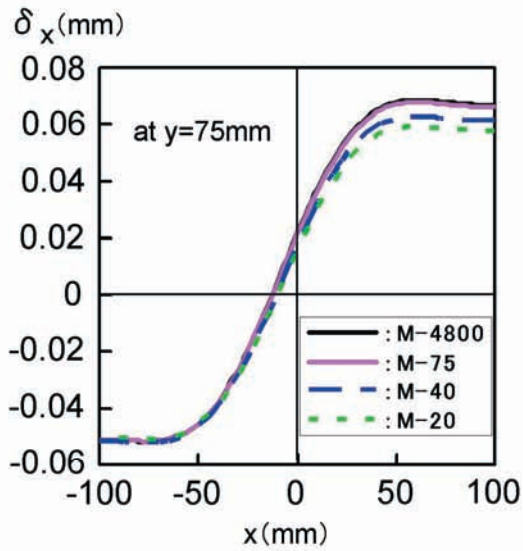


Fig. 14 Residual deformation δ_x (by new accurate method)

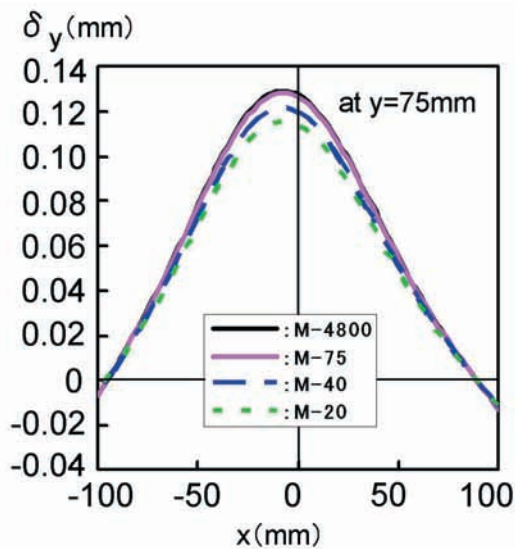


Fig. 15 Residual deformation δ_y (by new accurate method)

for the new theory was 75. The numbers of increments required to obtain accurate residual stress results were the same for both theories. The reduction ratio of the computation time was still 6.25%. For this deformation, the analytical results obtained by ABAQUS were almost identical with those obtained by the above two theories using 4800 increments

3.2.3 Limit of enlargement of temperature increment for accurate analysis

In the analysis by the new method, the accuracies of the transient stress and deformation results were the same as those of the residual results. They have not been included here owing to space limitations. In each element, if the stress point moved outside the yield surface after

some increments, it would be returned to the yield surface and satisfy the yield condition after the next increment. However, the accuracy clearly decreased when the temperature increment became very large (for example, when 20 increments were used), although the modifier of the new theory was very effective. The decrease was due to the difference in the temperature distribution history. When the temperature increment further increased, the difference between the histories for the very small increment and large increment also increased further. On the basis of the results of this study, the limit of the temperature increment is considered to be about 150°C. The history of the temperature distribution is the left important factor in shortening the computation time for accurate analysis.

4. Conclusion

The thermal elastic-plastic analysis of the transient and residual stresses and deformations that occur during welding require a long computation time because of the non-linearity of the mechanical behavior and the dependency on the temperature history. In this study, the thermal elastic and thermal elastic-plastic constitutive equations were modified to allow for the use of large temperature increments. Moreover, for the latter constitutive equation, the definition of the differential coefficient of the yield stress when the temperature changes was ingeniously modified to perfectly satisfy the yield condition.

A simple typical problem of thermal elastic-plastic mechanics was analyzed to verify the basic capability of the new theory. To examine the reliability and accuracy of the theory, a complex welding problem was also analyzed. The welding residual stress and deformation were analyzed by the new theory using large temperature increments. It was confirmed that the computation time was significantly shortened (reduced by one order) compared to those of the usual theory and ABAQUS, while maintaining high accuracy.

A new program or investment in much labor and time is not required for the new theory. The new constitutive equations can be easily introduced into the usual FEM program for thermal elastic-plastic analysis. This is another superior value of the new theory. Even if only Eq. (31) is applied, the accuracy will be largely improved. Only a few lines of the program need to be modified.

Nomenclature

Symbols

$[D^e]$: elastic matrix

$d[D^e]$: increment of elastic matrix

f : yield function

$f = 0$: yield surface

$df = 0$: consistency condition

H : strain-hardening coefficient

k : proportionality coefficient

$\{n\}$: outward unit vector normal to the yield surface at

the stress point

$\{n_\theta\}$: unit vector indicating the movement direction of the yield surface

T : temperature

dT : temperature increment

Greek Symbols

$\{\alpha\}$: instantaneous linear expansion coefficient

$\{\varepsilon^e\}$: total elastic strain

$\{d\varepsilon\}$: total strain increment

$\{d\varepsilon^T\}$: thermal strain increment

$\{d\varepsilon^e\}$: elastic strain increment

$\{d\varepsilon^P\}$: plastic strain increment

$\bar{\varepsilon}^P$: total magnitude of the plastic strain increment

$d\bar{\varepsilon}^P$: magnitude of the plastic strain increment

$\{\sigma\}$: stress

$\{d\sigma\}$: stress increment

$d\sigma_f$: normal component of $\{d\sigma\}$

σ_o : size of the yield surface

$d\sigma_o$: change in the size of the yield surface

$\{\theta\}$: center of the yield surface

$\{d\theta\}$: change in the center of the yield surface

References

- [1] Ueda, Y., and Yamakawa, T., 1971, "Analysis of Thermal Elastic-Plastic Stress and Strain during Welding by Finite Element Method," Transactions of the Japan Welding Society, 2(2), pp. 90-100.
- [2] Ueda, Y., and Nakacho, K., 1980, "Theory of Thermal Elastic-Plastic Analysis with a More General Work-Hardening Rule," Transactions of Joining and Welding Research Institute, Osaka University, 9(1), pp. 107-114.
- [3] Nakacho, K., 1985, "Theoretical Study on Welding Transient and Residual Stresses in Very Thick Joint and Their Reduction from Stress Relief Annealing," Dissertation, Osaka University.
- [4] Ueda, Y., Takahashi, E., Fukuda, K., and Nakacho, K., 1973, "Transient and Residual Stresses in Multi-Pass Welding," IIW (International Institute of Welding), Doc. X-698-73.
- [5] Ueda, Y., Takahashi, E., Fukuda, K., Sakamoto, K., and Nakacho, K., 1976, "Multipass Welding Stresses in Very Thick Plates and Their Reduction from Stress Relief Annealing," IIW, Doc. X-850-76.
- [6] Ueda, Y., Fukuda, K., Nakacho, K., Takahashi, E., and Sakamoto, K., 1976, "Transient and Residual Stresses from Multipass Weld in Very Thick Plates and Their Reduction from Stress Relief Annealing," ASME, Proc. 3rd International Conference on Pressure Vessel Technology, pp. 925-933.
- [7] Ueda, Y., Fukuda, K., and Nakacho, K., 1977, "Basic Procedures in Analysis and Measurement of Welding Residual Stresses by the Finite Element Method," TWI (The Welding Institute, Cambridge), International Conference on Residual Stresses in Welded Construction and Their Effects, Paper 3.
- [8] Ueda, Y., Nakacho, K., and Shimizu, T., 1984, "Improvement of Residual Stresses of Circumferential Joint of Pipe by Heat-Sink Welding for IGSCC," ASME, International PVP Conference, 84-PVP-10.
- [9] Ueda, Y., and Nakacho, K., 1985, "Three-Dimensional Welding Residual Stresses Calculated and Measured, TWI, International Conference on the Effects of Fabrication Related Stresses on Product Manufacture and Performance, Paper 32.
- [10] Ueda, Y., Nakacho, K., and Shimizu, T., 1986, "Improvement of Residual Stresses of Circumferential Joint of Pipe by Heat-Sink Welding," ASME, J. of Pressure Vessel Technology, 108, pp. 14-23.
- [11] Nakacho, K., and Ueda, Y., 1999, "A Simple Estimating Method for Reduction of Welding Residual Stresses in Thick Welded Joint from Stress-Relief Annealing - Part II," ASME, J. of Pressure Vessel Technology, 121, pp. 11-16.